

PEALD YSZ-based bilayer electrolyte for thin film-solid oxide fuel cells

This content has been downloaded from IOPscience. Please scroll down to see the full text.

2016 Nanotechnology 27 415402

(<http://iopscience.iop.org/0957-4484/27/41/415402>)

View [the table of contents for this issue](#), or go to the [journal homepage](#) for more

Download details:

IP Address: 220.149.124.192

This content was downloaded on 05/12/2016 at 06:15

Please note that [terms and conditions apply](#).

You may also be interested in:

[Nanoporous silver cathode surface-treated by atomic layer deposition of CeOx for low-temperature solid oxide fuel cells](#)

Ke Chean Neoh, Gwon Deok Han, Manjin Kim et al.

[Bias-assisted magnetron sputtering of yttria-stabilised zirconia thin films](#)

A A Solovyev, S V Rabotkin, I V Ionov et al.

[Direct-write microfabrication of single-chamber micro solid oxide fuel cells](#)

Melanie Kuhn, Teko Napporn, Michel Meunier et al.

[Ionic conductivity in oxide heterostructures: the role of interfaces](#)

Emiliana Fabbri, Daniele Pergolesi and Enrico Traversa

[Vertically oriented MoS2 nanoflakes coated on 3D carbon nanotubes for next generation Li-ion batteries](#)

Mumukshu D Patel, Eunho Cha, Nitin Choudhary et al.

[Atomic layer deposition of lithium phosphates as solid-state electrolytes for all-solid-state microbatteries](#)

Biqiong Wang, Jian Liu, Qian Sun et al.

[Preparation and Characterization of Anode-Supported YSZ Thin Film Electrolyte by Co-Tape Casting and Co-Sintering Process](#)

Q L Liu, C J Fu, S H Chan et al.

[Freeze-drying for sustainable synthesis of nitrogen doped porous carbon cryogel with enhanced supercapacitor and lithium ion storage performance](#)

Zheng Ling, Chang Yu, Xiaoming Fan et al.

PEALD YSZ-based bilayer electrolyte for thin film-solid oxide fuel cells

Wonjong Yu¹, Gu Young Cho¹, Soonwook Hong², Yeageun Lee²,
Young Beom Kim², Jihwan An³ and Suk Won Cha¹

¹ School of Mechanical and Aerospace Engineering, Seoul National University, San 56-1, Daehak dong, Gwanak-gu, Seoul 151-742, Korea

² Department of Mechanical Convergence Engineering, Hanyang University, Seoul 133-791, Korea

³ Manufacturing Systems and Design Engineering Program, Seoul National University of Science and Technology, Korea

E-mail: swcha@snu.ac.kr and jihwanan@seoultech.ac.kr

Received 2 June 2016, revised 12 July 2016

Accepted for publication 28 July 2016

Published 7 September 2016



CrossMark

Abstract

Yttria-stabilized zirconia (YSZ) thin film electrolyte deposited by plasma enhanced atomic layer deposition (PEALD) was investigated. PEALD YSZ-based bi-layered thin film electrolyte was employed for thin film solid oxide fuel cells on nanoporous anodic aluminum oxide substrates, whose electrochemical performance was compared to the cell with sputtered YSZ-based electrolyte. The cell with PEALD YSZ electrolyte showed higher open circuit voltage (OCV) of 1.0 V and peak power density of 182 mW cm^{-2} at 450°C compared to the one with sputtered YSZ electrolyte (0.88 V(OCV) , 70 mW cm^{-2} (peak power density)). High OCV and high power density of the cell with PEALD YSZ-based electrolyte is due to the reduction in ohmic and activation losses as well as the gas and electrical current tightness.

 Online supplementary data available from stacks.iop.org/NANO/27/415402/mmedia

Keywords: bilayer electrolyte, thin film, solid oxide fuel cell, plasma enhanced atomic layer deposition

(Some figures may appear in colour only in the online journal)

1. Introduction

Low temperature solid oxide fuel cell has been suggested for alleviating problems caused by high operating temperature (over 800°C) of conventional SOFCs such as high degradation rate, limited material selection, and low applicability for portable devices [1]. High ohmic loss caused by ionic transport and activation loss due to sluggish reaction at electrodes (anode and cathode) are the main reasons for the difficulty in lowering the operating temperature of SOFC [2]. Thus, to lower the operating temperature, nanoscale thin film electrolytes deposited by various deposition methods, e.g., sputtering, atomic layer deposition (ALD), and pulsed laser deposition (PLD), have been applied for the fabrication of thin film SOFCs [3, 4]. As the ohmic loss has been sufficiently decreased by applying thin film electrolytes, enabling operation of SOFCs at below 500°C , the activation loss at anode and cathode becomes major factor determining the

performance of the cells [3, 4]. Meanwhile, in order to fabricate nanoscale thin film electrolyte, substrates that could provide both mechanical strength and gas accessibility are necessary for the application in thin film SOFCs. The substrate for thin film SOFC, therefore, should have sufficient porosity for the facile access of gaseous fuel to the anode side and also should have mechanical strength to support the overlaid thin film membrane-electrode-assembly (MEA). In this regard, anodic aluminum oxide (AAO) substrates have been suggested for the fabrication of thin film SOFCs because of their scalability, reasonable thermo-mechanical strength and well-ordered porous structure [5].

Various vapor deposition methods have been applied for fabricating nanoscale thin film electrolyte. Sputtering and PLD are known as typical physical vapor deposition (PVD) methods for thin film fabrication and have been frequently used due to easy controllability of thin film microstructure and low deposition temperature. However, thin film

electrolytes deposited by PVD methods often suffer from pinhole issue causing the decrease in open circuit voltage (OCV) and the increase in leakage current. For instance, Kwon *et al* reported that it was hard to achieve pinhole-free electrolyte on porous substrate with less than 500 nm in thickness when PVD method were used for the thin film fabrication [6]. Contrariwise, ALD has been considered as promising tool for depositing pin-hole free nanoscale thin film. Using ALD, one can easily control the thickness of thin film at atomic scale and provide high density, uniformity, and step coverage for depositing large area due to sequential process with precursor and reactant [7, 8]. These characteristics of ALD enable the fabrication of pinhole-free electrolytes with high density and small grain size even on top of the highly rough nanoporous substrate. Despite all these advantages, low deposition rate ($\sim 1.0 \text{ \AA/cycle}$) and crystallinity have been pointed out as disadvantages of ALD. Plasma enhanced ALD (PEALD) has recently shown the potential for fabricating thin films with higher deposition rate, better crystallinity, and lower carbon contamination compared to conventional ALD (i.e., thermal ALD) [9–11]. Excited species such as ions and radicals in oxygen plasma used in PEALD enhance the chemical reactivity during deposition leading to improved film properties. Our group previously reported the fabrication of PEALD yttria-stabilized zirconia (YSZ) on AAO substrate with superior film properties in terms of density and gas tightness compared to thermal ALD YSZ [11].

In this study, PEALD YSZ thin film was applied to the fabrication of YSZ/yttria-doped ceria (YDC) bi-layer electrolyte on AAO substrate. Here, we report the successful fabrication of the SOFC with PEALD YSZ/sputter YDC bi-layer electrolyte and the effect of PEALD YSZ layer on the electrochemical performance of the SOFC. We think that the result presented in this study could provide a valuable insight for utilizing PEALD YSZ in fabricating high performance low-temperature thin film SOFCs.

2. Experimental

For the fabrication of YSZ/YDC bi-layer electrolyte cells, commercial AAOs having 80 nm pore size (Synkera, USA) were used as substrates. The thickness of AAO was $100 \mu\text{m}$. On top of AAO substrate, 8 mol % YSZ was deposited by using a showerhead type commercial PEALD apparatus (CN1, Atomic Premium, South Korea). Tris(methylcyclopentadienyl) yttrium and tetrakis(dimethylamido) zirconium were utilized as precursors for PEALD YSZ deposition. The temperatures of the canisters were controlled at $145 \text{ }^\circ\text{C}$ and $50 \text{ }^\circ\text{C}$ for yttrium and zirconium precursors, respectively. The lines for yttrium and zirconium precursors were heated to $155 \text{ }^\circ\text{C}$ and $70 \text{ }^\circ\text{C}$, and the substrate temperature was maintained at $250 \text{ }^\circ\text{C}$. Ar with 99.99% purity was supplied by 300 sccm for delivering the precursors to the substrate. Oxygen gas with 99.99% purity was supplied by 100 sccm as an oxidant. For plasma source, the power of oxygen plasma was maintained at 50 W, and both Ar 300 sccm and O_2 100 sccm were

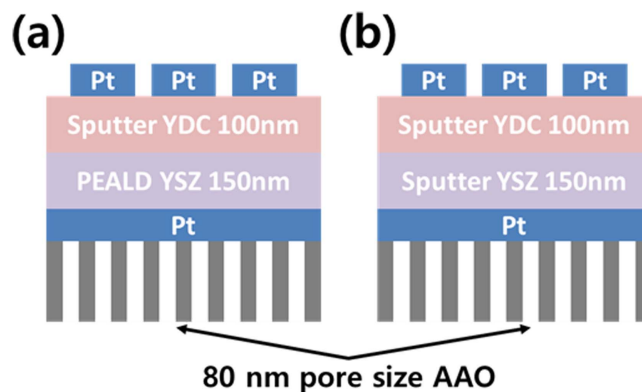


Figure 1. Schematic of bi-layered electrolyte thin film SOFCs structure deposited on 80 nm pore AAO substrate (a) PEALD YSZ/sputtered YDC (PEALD YSZ cell) (b) sputtered YSZ/YDC (sputter YSZ cell).

supplied to the chamber for plasma generation. Zirconia was deposited by repeating the sequence of precursor pulsing for 3 s, Ar gas purging for 30 s, O_2 oxidant pulsing for 1 s, plasma generation for 8 s, and Ar gas purging for 5 s. Yttria is deposited by repeating the sequence of precursor pulsing for 5 s, Ar gas purging for 60 s, O_2 oxidant pulsing for 1 s, plasma generation for 8 s, and Ar gas purging for 60 s. The doping ratio of yttria was controlled by changing the ratio of deposition cycles of yttria and zirconia. The ratio of yttria and zirconia PEALD cycles were set to be 1:7. The deposition rate of PEALD YSZ was calculated as 1.4 \AA/cycle .

For the fabrication of sputtered YSZ, YDC electrolytes and platinum (Pt) electrode, a commercial sputtering machine (A-Tech System Ltd, South Korea) was used to deposit YDC on top of PEALD YSZ/ sputtered YSZ, dense Pt on anode, and porous Pt on cathode. To deposit dense and porous Pt electrodes, chamber pressure of sputter was set to 5 mTorr and 90 mTorr, respectively [12, 13]. YSZ ($\text{Y}_{0.16}\text{Zr}_{0.84}$) metal and YDC (doping concentration of yttria: 20 mol %) ceramic targets were used for radio frequency (RF) magnetron sputtering. For YSZ and YDC deposition, 5 mTorr Ar and O_2 mixture gas atmosphere was set. Plasma power for YSZ and YDC was 200 W and 50 W, respectively. The deposition rate of YSZ and YDC was $\sim 100 \text{ nm h}^{-1}$ and $\sim 45 \text{ nm h}^{-1}$, respectively. Figure 1 shows the schematics of cross-sectional structures of two samples used in this study: 150 nm thick YSZ electrolyte by PEALD (hereafter called PEALD YSZ cell (figure 1(a)) and sputtering (hereafter called sputtered YSZ cell (figure 1(b)) were deposited on top of Pt anode on AAO substrate. YDC (100 nm thick) and porous Pt (80 nm thick) layers were sputtered subsequently on top of YSZ layers.

To investigate the composition and crystallinity of the samples, x-ray photoelectron spectroscopy (XPS)(AXIS, Kratos Analytical, Japan) and TEM (JEM-2100F, JEOL USA Inc., USA) were conducted. The compositions of the samples were investigated by XPS measurement. The surface of YSZ electrolyte was etched by Ar-ion at $1 \mu\text{A}$ current for 10 s to eliminate possible surface contamination. XPS analysis showed that the atomic concentrations of the PEALD YSZ

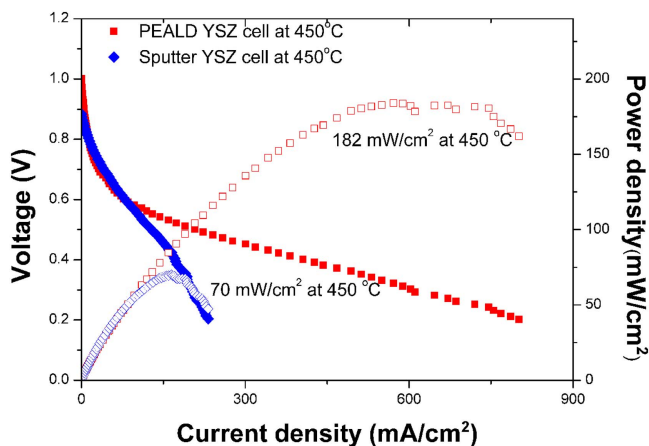


Figure 2. Polarization curves of PEALD YSZ and sputter YSZ cells measured at 450 °C.

thin film were Zr 3d = 34.8%, Y 3d = 4.9%, O 1s = 58.8%, and C 1s = 1.5%. From the XPS analysis, Y_2O_3 mole fraction (x ; from $(Y_2O_3)_x(ZrO_2)_{1-x}$) was confirmed as 8 mol%. The atomic concentrations of sputtered YSZ were Zr 3d = 25.4%, Y 3d = 4.8%, O 1s = 65.9%, and C 1s = 4.0%, and this analysis confirmed the Y_2O_3 mole fraction of 7.9 mol%. Field emission scanning electron microscopy (FESEM) (SUPRA 55VP, Carl Zeiss, Germany) and focused ion beam (FIB) (3D FEG, FEI Company, Netherland) were used for the characterization of the microstructure and surface grain size of the samples.

Electrochemical performance was measured by using a commercial test system (Gamry Potentiostats, Gamry Instruments)(FAS2, Gamry Instruments Inc., USA) with a customized test station. A micro probing system was applied for the test station to evaluate electrochemical performance. The temperature of the test station was controlled from at 450 °C. During the test, dry hydrogen was supplied by 20 sccm to the dense anode side, and the cathode side was exposed to the ambient air.

3. Results and discussion

The effect of PEALD YSZ layer on electrochemical performance for bi-layered electrolyte fabricated on AAO substrate was examined by comparing with sputter YSZ layer. Figure 2 shows current density (J)—voltage (V)—power density (P) behavior of the cells. The OCV of the PEALD YSZ cell was 1002 mV at 450 °C, which is close to the theoretical OCV at this temperature (~1100 mV), and was about 120 mV higher than that of the sputter YSZ cell (about 880 mV). The higher OCV of the PEALD YSZ cell implies that the PEALD YSZ layer may have better gas tightness and electron blockage compared to the sputtered YSZ layer.

The initial performance measurement of sputter YSZ cell showed the peak power density of $\sim 70 \text{ mW cm}^{-2}$. However, the voltage of sputter YSZ cell instantly dropped to zero right after the initial OCV measurement, possibly implying the electrically short circuit between anode and cathode. Such

low OCV of thin film SOFCs on porous substrate has been often reported when only PVD method was employed, which was due to pinholes stemming from nano pores of the substrate (e.g., AAO) [6]. Our results for sputtered YSZ cell also show that the pinhole free electrolytes could not be achieved if they are sputtered in nanoscale thickness. On the other hand, PEALD YSZ cell with the electrolyte fabricated by hybrid deposition method including PEALD showed 182 mW cm^{-2} peak power density (figure 2) and less than $\sim 2\%$ reduction of OCV during 1 h measurement.

To analyze the reason for the high OCV and the high power density of PEALD YSZ cell, electrochemical impedance spectroscopy (EIS) analysis was employed. Figure 3(a) shows the Nyquist plot of PEALD YSZ cell measured at different cell voltages (OCV, 0.8 V, and 0.6 V) at 450 °C. It is generally known that the ohmic resistance caused by ion and electron transports is independent of the cell voltage while the activation resistance is dependent on the cell voltage [14]. In figure 3, the intersect between the plot and the real (X) axis therefore means the ohmic resistance. In addition, the magnitude of two arcs shown in Nyquist plot, in general, is relevant to anode–electrolyte and cathode–electrolyte polarization processes if they show discernible changes depending on the cell voltage. Also the polarization resistance at cathode–electrolyte side is considered as larger than that at anode–electrolyte side due to the sluggish oxygen reduction reaction. In the magnified image of figure 3(a), the sizes of arcs changed with varying voltage conditions, which indicates they are associated with the polarization process. In order to verify the reason for the performance difference between the PEALD YSZ and the sputter YSZ cells, EIS of both cells measured at 0.6 V was compared in figure 3(b). The ohmic resistance of the PEALD YSZ cell was about $0.28 \Omega \text{ cm}^2$, which was almost 40% lower than that of the sputter YSZ cell (about $0.45 \Omega \text{ cm}^2$). The calculated ionic conductivities of both the PEALD YSZ and the sputter YSZ layers were about $8.9 \times 10^{-5} \text{ S cm}^{-1}$ and $5.6 \times 10^{-5} \text{ S cm}^{-1}$, respectively, which shows that the higher ionic conductivity of the PEALD YSZ electrolyte partly contributed to the high performance of the cell. Furthermore, it was clearly seen that the polarization resistance of the sputter YSZ cell was larger than that of the PEALD YSZ cell by about 42%. This result suggests that the high performance of the PEALD YSZ cell is largely due to the improved polarization process, especially at the cathode side.

Surface structure analysis for PEALD YSZ and sputter YSZ cells further confirms that the difference in surface morphology of YDC layer may have affected that in polarization process. Figure 4 shows FESEM images of YDC surface for PEALD YSZ and sputter YSZ cells. The images were analyzed by using image processing tool (Image-J) to calculate the average grain size and standard deviation. The analysis indicates that average grain sizes for YDC surfaces of PEALD and sputter YSZ cells were 15.2 nm and 20.8 nm, respectively, which indicates that the PEALD YSZ/YDC layer has a higher density of surface grain boundaries than the sputter YSZ/YDC layer. Surface grain boundaries at the cathode–electrolyte interface are known to be the preferential

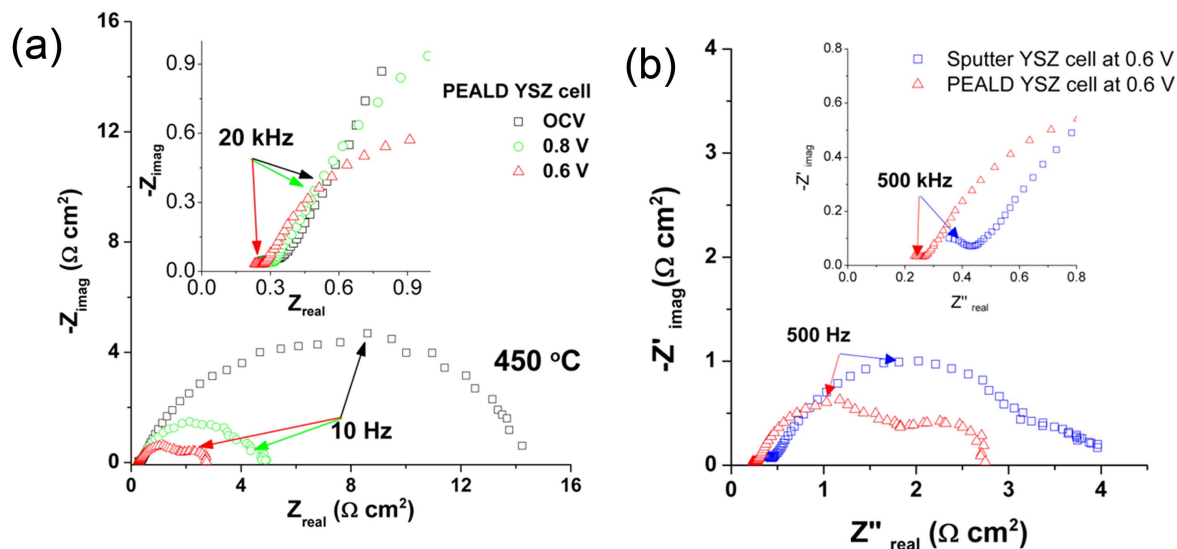


Figure 3. (a) Electrochemical impedance spectroscopy (EIS) of PEALD YSZ cell measured at open circuit voltage (OCV), 0.8 V, and 0.6 V. (b) Comparison of EIS analysis for PEALD and sputter YSZ cells at 0.6 V. Measurement was conducted at 450 °C.

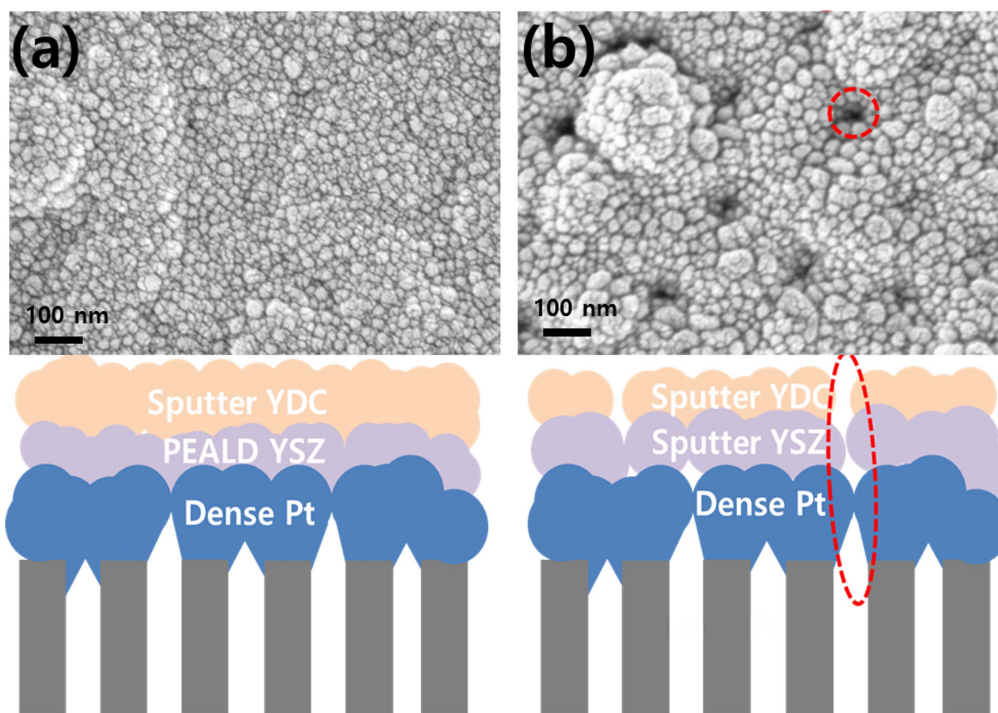


Figure 4. Field emission scanning electron microscope (FESEM) analysis for nanoscale surface structure of YDC electrolyte deposited on (a) PEALD YSZ and (b) sputter YSZ.

sites for oxygen ion incorporation due to the high local concentration of oxygen vacancies at grain boundaries. For example, Kim *et al* controlled the grain size of YDC cathodic interlayer with 400 nm thickness by annealing at 750 °C, 1100 °C, and 1300 °C, and showed that the cathodic polarization loss tend to increase as the temperature increases due to the grain growth [26]. In a similar way, we can speculate that the smaller grain size of YDC layer in PEALD YSZ cell at cathode–electrolyte interface may have resulted in lower cathodic polarization loss, leading to higher peak power density of the cell. Furthermore, figure 4 also shows that pinholes exist at the surface of YDC electrolyte in sputter

YSZ cell, which possibly due to the propagation of the pores of the AAO substrate. This result confirms that the low OCV of the sputter YSZ cell is indeed due to the gas permeation between anode and cathode. Meanwhile, the different nanoscale morphology of YDC layers at the cathode–electrolyte interface could be associated with the difference in the granular and/or crystal structure between PEALD YSZ and sputter YSZ electrolytes. Detailed study in this regard needs to be conducted and is currently in progress by our group.

Figure 5 shows FIB-SEM cross-sectional image of PEALD YSZ and sputter YSZ cells after operation at 450 °C for 1 h. It is notable that the sputtered YSZ layer partially

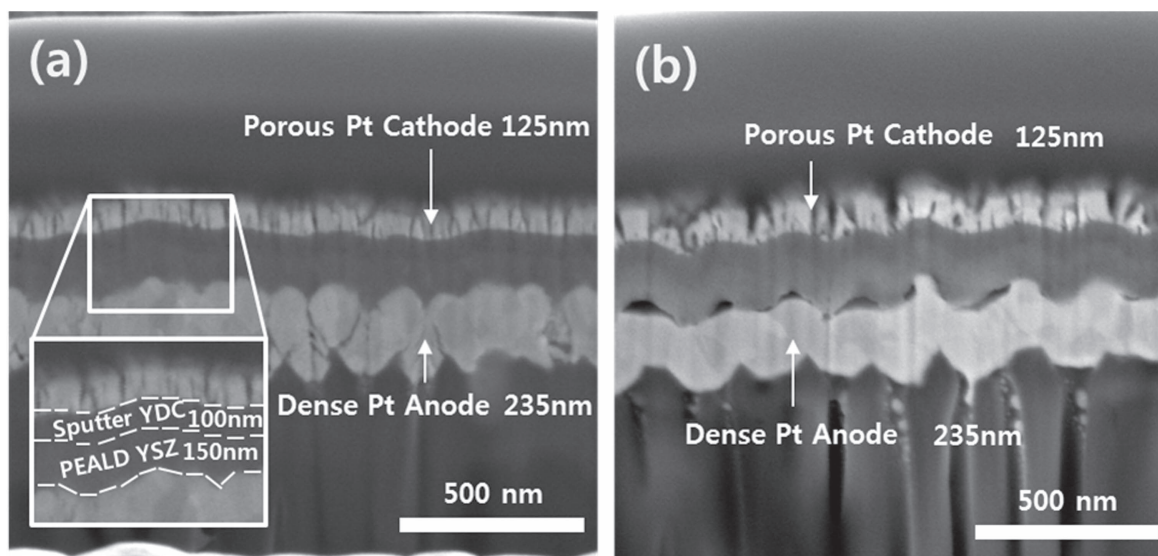


Figure 5. Cross-sectional focused ion beam (FIB) images of (a) PEALD and (b) sputter YSZ cells.

delaminated at the anode–electrolyte interface. Besides, structural damage was observed in porous cathode of sputter YSZ cell as well. This damage in the cathode could be due to the delamination of the underlying sputtered YSZ electrolyte. In multilayered thin film structure as in our samples, the stability of underlying layer could significantly affect the microstructure of upper layer. Gazzarri *et al* reported that the delamination of the electrode in SOFCs could cause an increase in both polarization and ohmic resistance by reducing the electrochemically active area [15]. FIB-SEM results shown here suggest that the higher polarization and ohmic resistances of sputter YSZ cell could be partly attributed to the defects at the interface and the structural damage of the cathode.

To further investigate the properties of PEALD YSZ electrolyte, transmission electron microscope (TEM) analysis was conducted. Polycrystalline nature of PEALD YSZ electrolyte was confirmed without visible defects, as is also shown in fast Fourier transform (FFT) analysis (figure 6). The lattice parameter (a) measured in the high-resolution TEM (HRTEM) image was about 0.513 ± 0.003 nm, which was comparable to the previously reported lattice parameter of 8 mol% YSZ (0.514 nm) [16]. HRTEM analysis confirms the superior film density and crystallinity of PEALD YSZ electrolyte, which may have led to the high ionic conductivity and, therefore, the low ohmic resistance.

4. Summary and conclusions

The effect of PEALD YSZ based bi-layered electrolyte on the electrochemical performance of thin film SOFC was studied by comparing with sputtered YSZ based bi-layered electrolyte. The cell with PEALD YSZ layer showed higher OCV than sputtered YSZ cell due to higher density and conformity providing gas tightness and electron blockage. EIS analysis indicated that ohmic and polarization resistances of the

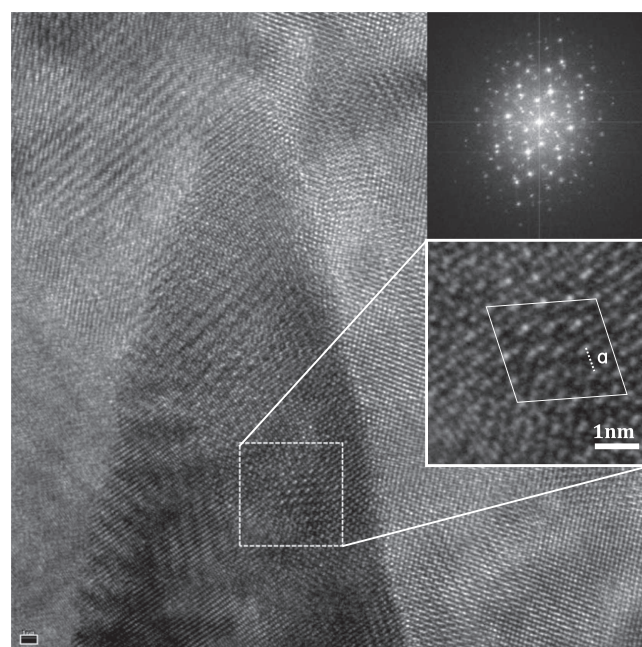


Figure 6. Transmission electron microscope (TEM) image of PEALD YSZ electrolyte and fast Fourier transform (FFT) images of PEALD YSZ electrolyte (inset).

PEALD YSZ cell were lower than those of the sputter YSZ cell. By employing FESEM analysis, it was confirmed that the grain size of the sputtered YDC electrolyte deposited on PEALD YSZ was smaller than that of the YSZ electrolyte deposited on sputter YSZ, which have resulted in the larger grain boundary density at the cathode–electrolyte interface and the improved surface exchange rate. We believe that the successful integration of PEALD YSZ electrolyte into the AAO-based thin film SOFC structure may have significant implications not only in fabricating high performance SOFCs but also in providing process solutions for efficient electrochemical devices based on thin film electrolytes.

Acknowledgments

This work was supported by the ‘New & Renewable Energy Core Technology Program’ of the Korea Institute of Energy Technology Evaluation and Planning (KETEP), granted financial resource from the Ministry of Trade, Industry & Energy, Republic of Korea. (No. 20153030040930)(KIST 2E26590).

References

- [1] Evans A, Bieberle-Hütter A, Rupp J L M and Gauckler L J 2009 Review on microfabricated micro-solid oxide fuel cell membranes *J. Power Sources* **194** 119–29
- [2] Steele B C and Heinzel A 2001 Materials for fuel-cell technologies *Nature* **414** 345–52
- [3] An J, Kim Y-B, Park J, Gür T M and Prinz F B 2013 Three-dimensional nanostructured bilayer solid oxide fuel cell with 1.3 W cm^{-2} at $450 \text{ }^\circ\text{C}$ *Nano Lett.* **13** 4551–5
- [4] Sasaki K 2002 Pt–perovskite cermet cathode for reduced-temperature SOFCs *Solid State Ion.* **148** 551–5
- [5] Kwon C-W, Lee J-I, Kim K-B, Lee H-W, Lee J-H and Son J-W 2012 The thermomechanical stability of micro-solid oxide fuel cells fabricated on anodized aluminum oxide membranes *J. Power Sources* **210** 178–83
- [6] Kwon C-W, Son J-W, Lee J-H, Kim H-M, Lee H-W and Kim K-B 2011 High-performance micro-solid oxide fuel cells fabricated on nanoporous anodic aluminum oxide templates *Adv. Funct. Mater.* **21** 1154–9
- [7] Shim J H, Kang S, Cha S-W, Lee W, Kim Y B, Park J S, Gür T M, Prinz F B, Chao C-C and An J 2013 Atomic layer deposition of thin-film ceramic electrolytes for high-performance fuel cells *J. Mater. Chem. A* **1** 12695
- [8] Elam J W, Dasgupta N P and Prinz F B 2011 ALD for clean energy conversion, utilization, and storage *MRS Bull.* **36** 899–906
- [9] Profijt H B, Potts S E, van de Sanden M C M and Kessels W M M 2011 Plasma-assisted atomic layer deposition: basics, opportunities, and challenges *J. Vac. Sci. Technol. A* **29** 050801
- [10] Cho G Y, Noh S, Lee Y H, Ji S and Cha S W 2014 Study of Y_2O_3 thin film prepared by plasma enhanced atomic layer deposition *ECS Trans.* **64** 15–21
- [11] Ji S, Cho G Y, Yu W, Su P-C, Lee M H and Cha S W 2015 Plasma-enhanced atomic layer deposition of nanoscale yttria-stabilized zirconia electrolyte for solid oxide fuel cells with porous substrate *ACS Appl. Mater. Interfaces* **7** 2998–3002
- [12] Park J, Lee Y, Chang I, Lee W and Cha S W 2015 Engineering of the electrode structure of thin film solid oxide fuel cells *Thin Solid Films* **584** 125–9
- [13] Park T, Cho G Y, Lee Y H, Tanveer W H, Yu W, Lee Y, Kim Y, An J and Cha S W 2016 Effect of anode morphology on the performance of thin film solid oxide fuel cell with PEALD YSZ electrolyte *Int. J. Hydrogen Energy* **41** 9638–43
- [14] An J, Kim Y-B and Prinz F B 2013 Ultra-thin platinum catalytic electrodes fabricated by atomic layer deposition *Phys. Chem. Chem. Phys.* **15** 7520–5
- [15] Gazzarri J I and Kesler O 2007 Non-destructive delamination detection in solid oxide fuel cells *J. Power Sources* **167** 430–41
- [16] Chiang Y, Kingery W and Birnie D 1997 Physical ceramics: principles for ceramic science and engineering (Wiley)